THE JOURNAL OF PHYSICAL CHEMISTRY C

Letter

Experimental Demonstration of the Mechanism of Light Harvesting Enhancement in Photonic-Crystal-Based Dye-Sensitized Solar Cells

Silvia Colodrero, Agustín Mihi, Juan A. Anta, Manuel Ocan#a, and Herna#n Míguez

J. Phys. Chem. C, **2009**, 113 (4), 1150-1154 • Publication Date (Web): 05 January 2009

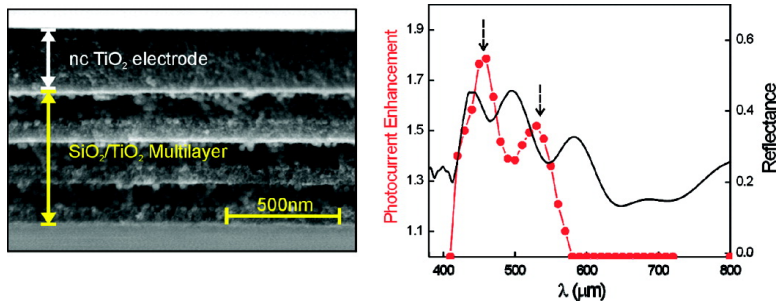

More About This Article

Additional resources and features associated with this article are available within the HTML version:

- Supporting Information
- Access to high resolution figures
- Links to articles and content related to this article
- Copyright permission to reproduce figures and/or text from this article

View the Full Text HTML

THE JOURNAL OF PHYSICAL CHEMISTRY C LETTERS

2009, *113,* 1150–1154
Published on Web 01/05/2009

Experimental Demonstration of the Mechanism of Light Harvesting Enhancement in Photonic-Crystal-Based Dye-Sensitized Solar Cells

Silvia Colodrero,[†] Agustín Mihi,[†] Juan A. Anta,[‡] Manuel Ocaña,[†] and Hernán Míguez*,[†]

Instituto de Ciencia de Materiales de Sevilla, Consejo Superior de Investigaciones Científicas, Américo Vespucio 49, 41092 Sevilla, Spain, and Departamento de Sistemas Físicos, Químicos y Naturales, Universidad Pablo de Olavide, 41013 Sevilla, Spain

Received: November 06, 2008; Revised Manuscript Received: November 27, 2008

Herein, we report an experimental analysis of the photogenerated current of very thin and uniform dye-sensitized nanocrytalline titanium oxide (nc-TiO_2) electrodes coupled to high-quality one-dimensional photonic crystals. The effect of well-defined optical absorption resonances are detected both in optical spectroscopy and photogenerated current experiments, a clear correspondence between them being established. Our study demonstrates that light trapping within absorbing electrodes is responsible for the absorption enhancement that has previously been reported and unveils the mechanism behind it. We prove that this effect improves significantly the power conversion efficiency of very thin electrodes.

Introduction

There is an increasing interest in the use of nanostructures to improve solar energy conversion devices.[1] In this context, a few experiments have been recently reported on the effect of coupling a photonic crystal to an absorbing electrode. Enhancement of light harvesting efficiency has been demonstrated in silicon[2] and dye-sensitized solar cells[3,4] (DSSC) using three-dimensional photonic crystals as coherent scattering layers. More importantly, an enhancement of the power conversion efficiency has been observed in DSSC coupled to a highly reflecting nanoparticle-based one-dimensional photonic crystal (1D PC).[5] The physical mechanism of enhancement has been thoroughly analyzed theoretically[6] and partially confirmed experimentally.[7] Enhancement of optical absorption is primarily due to the partial localization of photons of certain narrow frequency ranges within the absorbing layer as a result of its coupling to the photonic crystal, which acts as a porous low-loss dielectric mirror.[6] These optical modes could, in principle, be recognized as narrow dips in the reflectance spectra at frequencies located within the photonic band gap[8] or, alternatively, as the corresponding peak in the spectral dependence of the photocurrent. However, since most of the electrodes so far tested are nonuniform in thickness and their average width is above 2 μm, the number of localized modes is large, and its spectral position changes from place to place, giving rise to a spectral overlap that has not allowed identification of them separately.

Herein, we report an experimental analysis of the photogenerated current of very thin and uniform dye-sensitized nanocrystalline titanium oxide (nc-TiO_2) electrodes coupled to high-quality one-dimensional photonic crystals. The effect of well-defined optical absorption resonances is detected both in optical spectroscopy and photogenerated current experiments, an unambiguous correspondence between them being established. These results confirm that photon resonances within absorbing electrodes are responsible for the light harvesting enhancement that has previously been reported in photonic-crystal-based solar cells. Besides, we prove that this effect improves the power conversion efficiency of very thin electrodes, enhancement factors between 2 and 6 being attained in photonic-crystal-based solar cells when compared to reference electrodes.

Experimental Section

Nanoparticle Synthesis. Nanocrystalline TiO_2 particles are synthesized by using a procedure reported by Burnside et al. based on the hydrolysis of titanium isopropoxide followed by a peptization process under hydrothermal conditions,[9] which was slightly modified. In our case, 20 mL of titanium isopropoxide (97% Aldrich) was added to 36 mL of Milli-Q water and stirred for 1 h. Once the alcoxide was hydrolyzed, the product was filtered using 1.2 μm RTTP Millipore membranes, washed several times with distilled water, and placed in a Teflon reactor with 3.9 mL of an aqueous solution (0.6 M) of tetramethylammonium hydroxide (Fluka). After homogenizing the suspension with a stir bar, the reactor was placed in a oven preheated at 120 °C, where it was kept for 3 h. After this, a colloidal suspension of titanium oxide crystallites with an anatase structure, as confirmed by X-ray diffraction, was obtained. Later, centrifugation at 14 000 rpm for 10 min allowed elimination of some large aggregates from the dispersion. A rather narrow distribution of nanocrystals centered at 5 nm was achieved after this process, as checked by photocorrelation spectroscopy and transmission electron microscopy measurements. Silicon oxide nanoparticles (20 nm) were purchased from Dupont (LUDOX TMA colloidal silica, 34 wt % suspension in H_2O). TiO_2 or SiO_2 nanoparticles were suspended in a mixture of water (21 vol %) and methanol (79 vol %) in order to be used as precursors for the spin-coating process leading to the formation of the 1D PC within the cell.

* To whom correspondence should be addressed. E-mail: hernan@icmse.csic.es.
[†] Consejo Superior de Investigaciones Científicas.
[‡] Universidad Pablo de Olavide.

10.1021/jp809789s CCC: $40.75

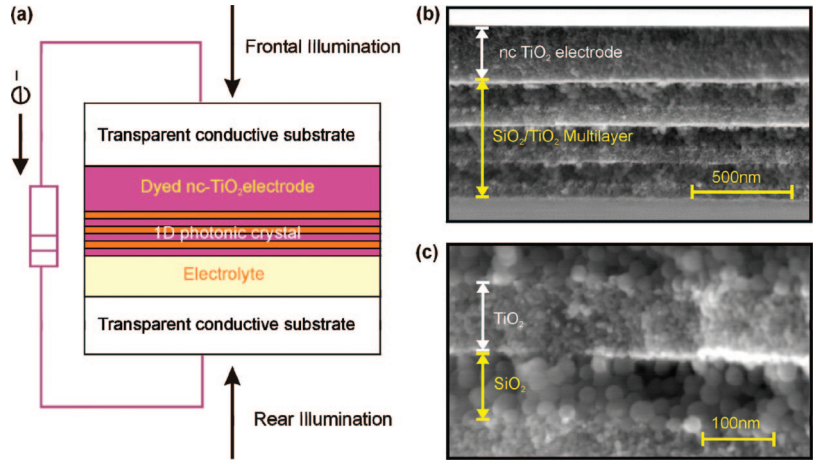

Figure 1. (a) Scheme of a dye-sensitized solar cell coupled to a 1D photonic crystal showing illumination both through the dye-coated TiO_2 layer (front illumination) and through the counter electrode (rear illumination). (b) FESEM image of a cross section of the nanocrystalline titanium dioxide electrode (vertical white line) coupled to the porous SiO_2-TiO_2 multilayer (vertical yellow line). (c) Magnified view of the different types of particles of which the multilayer is made. The spherical particles of silica and the smaller crystallites of titania can be clearly seen.

Fabrication and Structural Characterization of the Solar Cell Containing a 1D Photonic Crystal. First, a layer of the above-mentioned nanocrystalline TiO_2 particles was deposited onto a 25 mm × 25 mm conducting transparent substrate (FTO coated glass, Hartford Glass, Inc.) by a combination by the doctor blade technique, spin-coating, or a combination of both. A course rough layer was attained through the former, but a uniform and smooth surface was achieved in the final coating after a drop of a suspension of fine titania particles was spun onto it. For this work, the total thickness ranged between 300 nm and 1500 nm. Then, in order to build the Bragg reflector onto this coated substrate, layers of silica and the same nc-TiO_2 particles were deposited alternately by spin-coating 250 μL drops of their colloidal suspensions. For most cells, the titania-coated conducting substrate was spun at 100 revolutions per second (rps). Periodic multilayers of different lattice parameter were attained by keeping the TiO_2 nanocrystal concentration constant at 5 wt % and changing the silica concentration within the range between 1 and 5 wt %.[10] The PC properties of this structure are evident to the naked eye already with four layers deposited due to the high dielectric contrast between the two types of constituent layers. In most cases, a six-layer stack was built. After this, the multilayer coated substrate was thermally annealed at 450 °C in order to sinter the titania nanocrystals and remove all water bonded to the particles surface. When the temperature reached 120 °C during the cooling down process, the structure was removed from the furnace and immersed in a 0.025 wt % solution of ruthenium bypiridile dye (ruthenium 535-bis TBA, Solaronix) in ethanol overnight in order to ensure a proper adsorption of the dye on the nc-TiO_2 surface. After this, the electrode was put into electrical contact with a platinum (Pt catalyst T/SP, Solaronix) covered counter electrode by infiltrating a liquid electrolyte in between them. The employed electrolyte was composed of 100 mM I_2 (Aldrich, 99.999%), 100 mM LiI (Aldrich, 99.9%), 600 mM $[(C_4H_9)_4N]I$ (Aldrich, 98%), and 500 mM 4-tert-butylpyridine (Aldrich, 99%). The solvent used in this case was 3-methoxy propionitrile (Fluka, ≥99%). The porous nature of the periodic multilayer allows the electrolyte to soak the sensitized nc-TiO_2 coating. Previously, a thin hot-melt polymeric window (Surlyn, 1702 Dupont) that softens at 120 °C was used as a spacer and to seal the cell at the same time. Cross sections of the cell were imaged using a field emission scanning electron microscope (Hitachi 5200) operating at 5 kV and without using any conducting coating.

Optical Reflectance Measurements. Optical characterization was performed using a Fourier transform infrared spectrophotometer (Bruker IFS-66) attached to a microscope and operating in reflection mode. A ×4 objective with a numerical aperture of 0.1 (light cone angle ± 5.7°) was used to irradiate the solar cell and collect the reflected light at quasi-normal incidence with respect to its surface. A spatial filter was used to selectively detect light from 1 mm^2 circular regions of the sample.

Photoelectric Measurements. Incident photon to electric current conversion efficiencies (IPCE) were measured in the spectral range between 400 and 800 nm, illuminating the front side of the cell with a plane parallel beam coming from a 450 W xenon lamp (Oriel) after being dispersed by a monochromator (Oriel) containing a 1200 lines/mm grating (Oriel). Slits were chosen to attain a 10 nm wavelength resolution. A silicon photodiode (Thorlabs) of known response was used as a reference to extract the IPCE curves. *IV* curves were measured under white light illumination coming from the same light source plus UV and water IR filters. Currents were registered via a battery-operated potentiostat. A mask of 1 mm^2 was used in order to perform the photoelectric characterization from the same areas from which the reflectance spectra were obtained.

Results and Discussion

Figure 1 displays both a scheme and field emission scanning electron microscope images of a cross section of the dye-sensitized solar cell employed to perform the experiments herein reported. The electrode thickness used in this work is between 300 and 1500 nm, much thinner than those typically employed in standard solar cells.[11,12] The nanoparticle multilayer is periodic at distances on the order of the tens of nanometers and porous at the mesoscale, as has been thoroughly described somewhere else.[10] The thickness of these layers is controlled through either the concentration of the precursor suspension (typically between 1 and 5 wt %) or the rotation speed of the substrate (typically between 100 and 150 revolutions per second, rps) during a spin-coating process. Typical achievable values are in the range of 10−200 nm, although the minimum film thickness varies as a function of the particle size in suspension and its ease to disperse. The nanoparticle multilayer behaves as a one-dimensional photonic crystal or distributed Bragg reflector that

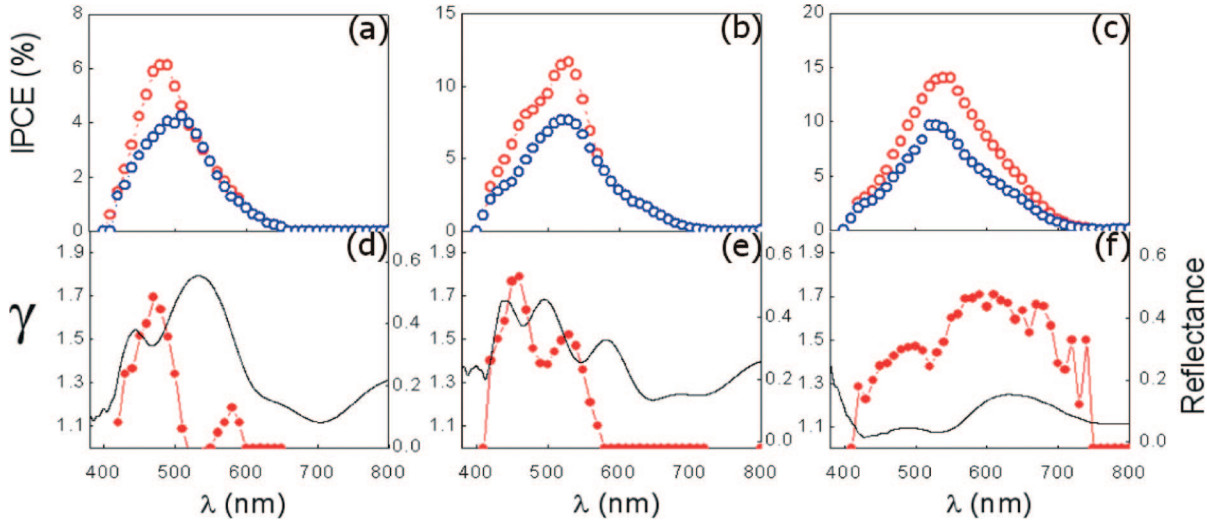

Figure 2. Incident photon to current conversion efficiency (IPCE, %) versus wavelength for cells containing the same 1D photonic crystal coupled to a dye-sensitized nc-TiO_2 layer of different thicknesses in each case (red circles). For comparison, we plot the IPCE for the same dye-sensitized nc-TiO_2 layers without the photonic crystal (blue circles). (a) A 350 nm nc-TiO_2 film, (b) a 600 nm nc-TiO_2 film, and (c) a 1500 nm nc-TiO_2 film. All of them are coupled to a 6 ML 1D photonic crystal (65 ± 5 nm SiO_2, 85 ± 5 nm nc-TiO_2). (d), (f), and (g) show the reflectance spectra of the 1D PC-based solar cell (solid line) and the photocurrent enhancement factor γ (red circles), defined as the ratio between the IPCE of the 1D PC-based cell and that of the standard for the systems described in (a), (b), and (c), respectively.

is able to efficiently localize incident radiation within the dye-sensitized nc-TiO_2 layer. It has been proven that this effect causes a significant enhancement of the power conversion efficiency of standard DSSC.[5] In order to observe this effect light must encounter first the absorbing layer and then the photonic crystal, that is, cells must be illuminated from the anode (front-side illumination).

The spectral response of the incident photon to current conversion efficiency (IPCE) is plotted in Figure 2 for three DSSCs having different dye-sensitized nc-TiO_2 electrode thicknesses but the same 1D PC implemented. Electrode thickness was optically controlled in all cases, which allowed us to build reference standard cells (that is, without a 1D PC implemented) with the exact same characteristics, as shown in the Supporting Information. Figure 2a−c displays the IPCE measured for the 1D PC-containing cells (red open circles) versus the corresponding standard cells (blue open circles). In all cases, the PC-based cells show a much higher short circuit photocurrent than the standard one for a certain wavelength range. Please notice that there is no contribution of the nc-TiO_2 layers forming the 1D PC to the photoconductivity since they are separated by insulating SiO_2 layers. In each case, an enhancement factor γ was calculated as the ratio between the IPCE of the 1D PC-based cell and that of the standard one. The spectral behavior of γ for each cell is shown in Figure 2d−f, where they are also compared to their optical reflectance measured under front-side illumination. It can be clearly seen that peaks of the photocurrent correspond to the dips in reflectance, which are the fingerprint of optical resonant modes localized in a film coupled to a photonic crystal, as it has been thoroughly analyzed before.[8,13] Those resonant frequencies are partially localized within the electrode, thus increasing its residence time in the absorbing layer and hence their probability of being absorbed.[6] In the reflectance spectrum plotted in Figure 2d, for instance, we can clearly distinguish the presence of one localized mode and one photocurrent peak at the same spectral position. The electrode thickness is 350 nm in this case. As we increase the thickness of the dye-sensitized electrode, the number of localized modes rises and so does the number of peaks in the γ curve. In the example shown in Figure 2e, an electrode thickness of 600 nm gives rise to two partially localized modes within the band gap. In the cell selected for Figure 2f, the electrode thickness is 1500 nm and individual resonances can no longer be distinguished. In this latter case, the IPCE is enlarged along the full width of the band gap, which roughly coincides with the full absorption band of the ruthenium dye. This match is only possible due to the large dielectric contrast between the SiO_2 and nc-TiO_2 layers that yields a wide photonic band gap (the refractive index of each layer is estimated from the fitting of the optical properties to be $n_{SiO_2} = 1.46$ and $n_{nc\text{-}TiO_2} = 2.03$ after electrolyte infiltration). The presence of a photonic crystal not only enhances the photogenerated current but also allows one to vary the spectral photoelectric response of thin electrodes in a controlled manner. In the example shown in Figure 2a, the largest current is attained at $\lambda = 470$ nm instead of at $\lambda = 515$ nm, where the dye absorption curve reaches its maximum. Thus, the photonic crystal allows tailoring to measure the enhanced absorption window of the dye, and thus, its overlap with the solar spectrum. This opens the way to utilize other dyes with lower extinction coefficients in the visible range but with better adsorption and electrochemical features. In addition, other electrolytes may be used, provided charge diffusion through the multilayered photonic crystal is carefully optimized.

We would like to highlight that the results shown in Figure 2 constitute the first direct experimental evidence of the coexistence of photocurrent resonances and optical resonances in photonic-crystal-based DSSCs. They have previously been predicted by us as the source of light harvesting enhancement based only on theoretical considerations and on indirect experimental evidence of us and others. Although similar effects to those reported by T. Mallouk et al. in ref 3 have been observed for other types of photovoltaic cells coupled to photonic crystals, such as silicon electrodes coupled to opals,[2] no experimental observation of the link between photocurrent peaks and optical resonances has been presented so far. The reason for this lies on the strict planarity and small thickness restrictions imposed on the electrode in order to allow clear identification of individual optical resonances.

Insight on the mechanism of enhancement can be extracted from the analysis of the optical response of the solar cells. The

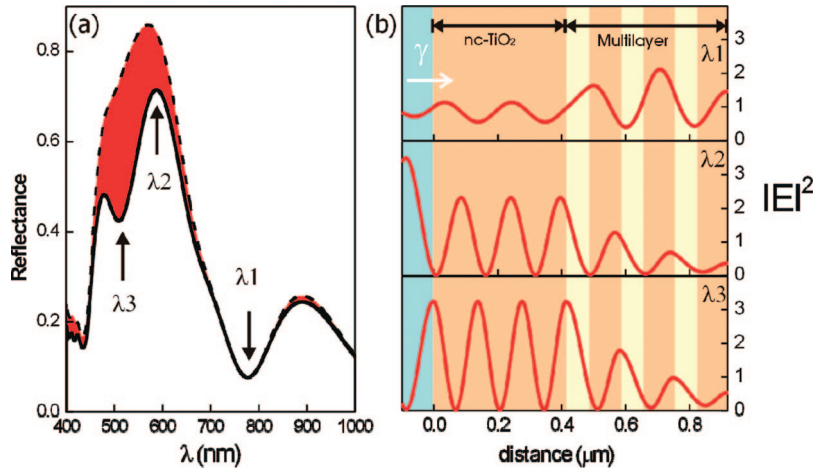

Figure 3. Optical response of the dye-sensitized electrode coupled to a porous nanoparticle-based 1D photonic crystal. (a) Reflectance spectra of a 415 nm thick film of nc-TiO_2 followed by a 3 period thick 1D photonic crystal composed of 95 ± 5 nm of silica and 75 ± 5 nm of titania films measured under front (solid line) and rear (dashed line, shaded in red) illumination conditions. (b) Spatial distribution of the square amplitude of the electric field of the system described in (a) at three selected wavelengths from the spectrum attained for front-illumination conditions, as obtained from the scalar wave approximation based fittings of the experimental reflectance. At the pass band, $\lambda_1 = 0.775$ μm; at a maximum of the reflectance peak, $\lambda_2 = 0.575$ μm; and at the dip in the reflectance peak, $\lambda_3 = 0.512$ μm.

optical response of the electrode coupled to a 1D PC is asymmetric, as illustrated in Figure 3a, where we show the reflectance spectra of the photonic-crystal-based dye-sensitized cell when illuminated in front (solid line) and rear (dashed line, red shaded curve) configurations. In the latter case (rear illumination), incident photons encounter the 1D PC first, and the optical response is then similar to that of the nanostructured multilayer alone, an intense reflection peak at photonic band gap frequencies being observed. However, when light impinges from the electrode side (front illumination, in the convention that we have adopted), a well-pronounced dip within photonic band gap frequencies is detected. For these modes, the dye-sensitized nc-TiO_2 electrode acts as a resonant cavity in which photons are localized, as illustrated in Figure 3b. Fitting of the experimental spectra using a scalar wave approximation[14] allowed us to calculate the spatial distribution of the squared electric field for three selected frequencies impinging under front-illumination conditions. Results are plotted in Figure 3b. It can be clearly seen that at the spectral position where the dip in reflectance attributed to a surface resonant mode is found (λ_3), localization is stronger within the electrode than that for frequencies spectrally located outside of the band gap (λ_1) or at the top of the reflectance peak (λ_2). This example shows that dips in reflectance within the band gap region are the fingerprint of partially localized modes within the electrode, arising due to the presence of the photonic crystal. For these modes, matter−radiation interaction times are much longer; thus, the probability of optical absorption, and therefore the photogenerated current, is expected to be enhanced. Notice that the field intensity within the electrode for those frequencies lying within the spectral band gap width but not affected by localization (λ_2) is also increased as a result of being back-reflected by the 1D PC. Hence, although less efficient, it constitutes a second enhancement mechanism provided by the 1D PC.

In order to evaluate the effect of these resonant absorptions on the power conversion efficiency, η, of the electrode, the change of the current density against the voltage bias was also tested in simulated sunlight (100 mW/cm^2) for the 1D PC-based solar cells and compared to their respective references. Results are shown in Figure 4a for a 350 nm thick dye-sensitized nc-TiO_2 electrode coupled to photonic crystals of lattice parameters 140 ± 10 (blue diamonds) and 180 ± 10 nm (green squares).

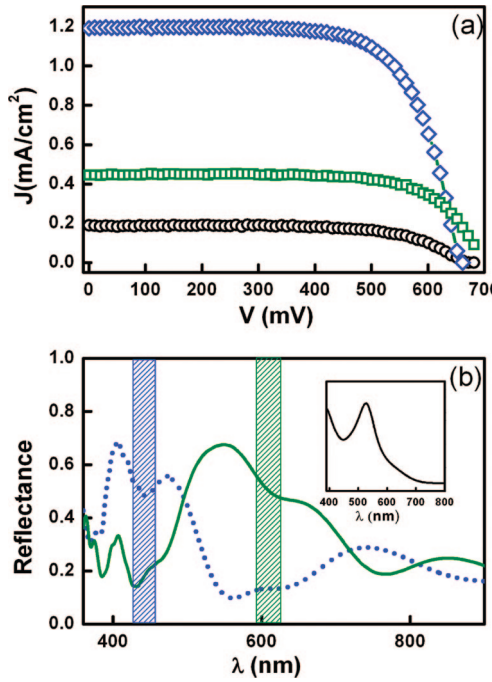

Figure 4. (a) Current voltage curves under 1 sun illumination (100 mW/cm^2) of a 350 nm thick dye-sensitized nc-TiO_2 electrode coupled to different 1D photonic crystals. The lattice parameter in each case is 140 ± 10 (blue diamonds) and 180 ± 10 nm (green squares). In all cases, the TiO_2 layer thickness is around 85 ± 5 nm. The *IV* curve of a reference cell with the same electrode thickness is also plotted (black circles). (b) Specular reflectance spectra of each one of the PC-based solar cells mentioned in (a) after measuring under front illumination. It can be observed that dips in the reflectance are obtained at different wavelengths. This indicates that the localization of those frequencies within the absorbing electrode can be modified depending on the photonic crystal built on top of it. The absorption band of the ruthenium bypiridile dye (in arbitrary units) is shown in the inset.

The *IV* curve of a reference cell is also shown for comparison (black circles). It can be clearly seen that all 1D PC-based cells show a much better performance than the reference. J_{sc} is improved without lowering V_{oc} since the charge-transport, injection, and recombination kinetics are not affected, in a first approximation, by the presence of the photonic crystal. This factor greatly contributes to the extraordinarily large enhance-

ment of η achieved. From the *IV* curves, we calculated $\eta = (\mathrm{ff} \times J_{sc} \times V_{oc})/P_i$, where ff is the fill factor, J_{sc} is the absolute value of the current density at short circuit, V_{oc} is the photovoltage at open circuit, and P_i is the incident light power density. For the examples selected for Figure 4a, η rises from $\eta_{ref} = 0.083\%$ to $\eta_{PC1} = 0.221\%$ and $\eta_{PC2} = 0.548\%$, depending on the spectral range at which the 1D PC used presents its reflectance maximum. For the sake of comparison, optical reflectance spectra of these two PC-based cells under analysis are plotted in Figure 4b. The position of the absorption resonance is highlighted in each case by a vertical bar, and the absorption band of the dye is shown in the inset. Interestingly, the larger enhancement is attained for the photonic-crystal-based cell in which the optical absorption resonance coincides with the dye absorption maximum. This is a direct consequence of using very thin electrodes that are unable to capture all photons at those wavelengths.

These results demonstrate that the effect of the coupling between a thin electrode and a 1D photonic crystal on the power conversion efficiency of the former is dramatic, η increasing more than six times with respect to the reference value in the optimum case. It should be noted that this effect is not as significant for thicker standard electrodes,[5] for which enhancement factors between $\gamma = 1.15$ and 1.3 have been reported when coupled to 1D PCs. Given a certain photonic crystal coupled to a DSSC, the thicker the electrode, the larger the number of resonant modes within the absorbing layer. However, this does not mean that the enhancement factor is larger in the cell with the thicker electrode. Thin electrodes present a much larger optical transmission, and much fewer photons are absorbed than in thick ones. Thus, the effect of coupling a photonic crystal on the light harvesting efficiency is much larger for thin than that for thick electrodes, independent of the number of resonant modes. In other words, the creation of one resonant mode within a thin electrode can give rise to a much larger enhancement factor than the creation of many into a thick one, for the simple reason that weak signals are much more efficiently amplified than strong ones. This by no means implies that the absolute efficiency is necessarily larger in thin than that in thick electrodes. In fact, we have shown that similar photonic crystals give rise to an enhancement factor of $\gamma = 1.15$ in a 7.5 μm thick dye-sensitized layer[5] and to one of $\gamma = 6$ in a 0.35 μm thick one. It implies that a thick DSSC shows an increase of power conversion efficiency from 4 to 4.6% when coupled to a photonic crystal, while the increase for the thin electrode will be from 0.1 to 0.6%. These low-efficiency values are due to the small thickness of the electrodes employed, a necessary condition to observe individual optical and photocurrent resonances. These values highlight the potential that nanoparticle-based photonic crystals might have in other cells using very thin absorbing layers, in which the main source of loss of efficiency is frequently the low amount of light absorbed.

Conclusions

The results herein presented confirm experimentally that photon resonances occurring within absorbing electrodes are responsible for the enhancement of light harvesting efficiency that has repeatedly been reported in solar cells integrating photonic crystals as scattering layers. Well-defined optical absorption resonances are identified in the reflectance of the cell, and its amplifying effect on the photogenerated current at targeted wavelengths is unambiguously established. We also prove that this effect largely improves the power conversion efficiency of thin electrodes.

Acknowledgment. This work has been funded by the company Nanologica AB, the Spanish Ministry of Science and Education under Grants MAT2008-02166/NAN and ENE2007-01657, and project HOPE CSD2007-00007 (Consolider-Ingenio 2010).

Supporting Information Available: Nc-TiO_2 electrodes were made by spin-coating and measured optically, which allowed us to control the thickness and compare the effect of coupling 1D PCs onto them. This material is available free of charge via the Internet at http://pubs.acs.org.

References and Notes

(1) Kamat, P. V. *J. Phys. Chem. C* **2007**, *111*, 2834.
(2) O'Brien, P.; Kherani, N. P.; Zukotynski, S.; Ozin, G. A.; Vekris, E.; Tetreault, N.; Chutinan, A.; John, S.; Mihi, A.; Míguez, H. *Adv. Mater.* **2007**, *19*, 4177.
(3) Nishimura, S.; Abrams, V.; Lewis, B. A.; Halaoui, L.; Mallouk, T. E.; Benkstein, K. D.; Lagemaat, J.; Frank, A. J. *J. Am. Chem. Soc.* **2003**, *125*, 6306.
(4) Rodriguez, I.; Atienzar, P.; Ramiro-Manzano, F.; Meseguer, F.; Corma, A.; Garcia, H. *Photonics and Nanostructures—Fundamentals and Applications* **2005**, *3*, 148.
(5) Colodrero, S.; Mihi, A.; Häggman, L.; Ocaña, M.; Boschloo, G.; Hagfeldt, A.; Míguez, H. *Adv. Mater.* Published online. DOI: 10.1002/adma.200703115.
(6) Mihi, A.; Míguez, H. *J. Phys. Chem. B* **2005**, *109*, 15968.
(7) Mihi, A.; Calvo, M. E.; Anta, J. A.; Míguez, H. *J. Phys. Chem. C* **2008**, *112*, 13.
(8) Mihi, A.; Míguez, H.; Rodríguez, I.; Rubio, S.; Meseguer, F. *Phys. Rev. B* **2005**, *71*, 125131.
(9) Burnside, S. D.; Shklover, V.; Barbe, C.; Comte, P.; Arendse, F.; Brooks, K.; Grätzel, M. *Chem. Mater.* **1998**, *10*, 2419.
(10) Colodrero, S.; Ocaña, M.; Míguez, H. *Langmuir* **2008**, *24*, 4430.
(11) O'Regan, B.; Grätzel, M. *Nature* **1991**, *353*, 737.
(12) Grätzel, M. *Inorg. Chem.* **2005**, *44*, 6841.
(13) Arsenault, A. C.; Halfyard, J.; Wang, Z.; Kitaev, V.; Ozin, G. A.; Manners, I.; Mihi, A.; Míguez, H. *Langmuir* **2005**, *21*, 499.
(14) Shung, K. W. K.; Tsai, Y. C. *Phys. Rev. B* **1993**, *48*, 11265.

JP809789S